Published in final edited form as:
Cell. 2011 December 9; 147(6): 1324–1339. doi:10.1016/j.cell.2011.10.045.

Loss of Tankyrase-mediated destruction of 3BP2 is the underlying pathogenic mechanism of cherubism

Noam Levaot[1,*], **Oleksandr Voytyuk**[1,*], **Ioannis Dimitriou**[1], **Fabrice Sircoulomb**[1], **Arun Chandrakumar**[1], **Marcel Deckert**[2], **Paul M. Krzyzanowski**[1], **Andrew Scotter**[1], **Shengqing Gu**[1], **Salima Janmohamed**[1], **Feng Cong**[3], **Paul D. Simoncic**[1], **Yasuyoshi Ueki**[4], **Jose La Rose**[1], and **Robert Rottapel**[1,5]

[1]Ontario Cancer Institute and the Campbell Family Cancer Research Institute, 101 College Street, Rm 8-703 Toronto Medical Discovery Tower, University of Toronto, Toronto, Ontario, Canada, M5G 1L7

[2]INSERM, UMR576, University of Nice, Sophia-Antipolis, Nice, F-06202 France

[3]Developmental and Molecular Pathways, Novartis Institute of Biomedical Research, Cambridge, MA 02139, USA

[4]University of Missouri-Kansas City, School of Dentistry 650 E 25th Street, Room 3143, Kansas City, MO 64108

[5]Saint Michael's Hospital, Division of Rheumatology, Department of Medicine, 30 Bond Street, Toronto, Ontario, Canada

Summary

Cherubism is an autosomal dominant syndrome characterized by inflammatory destructive bony lesions resulting in symmetrical deformities of the facial bones. Cherubism is caused by mutations in *Sh3bp2*, the gene that encodes the adaptor protein 3BP2. Most identified mutations in 3BP2 lie within the peptide sequence RSPPDG. A mouse model of cherubism develops hyperactive bone remodelling osteoclasts and systemic inflammation characterized by expansion of the myelomonocytic lineage. The mechanism by which cherubism mutations alter 3BP2 function has remained obscure. Here we show that Tankyrase, a member of the poly(ADP-ribose)polymerase (PARP) family, regulates 3BP2 stability through ADP-ribosylation and subsequent ubiquitylation by the E3-ubiquitin ligase RNF146 in osteoclasts. Cherubism mutations uncouple 3BP2 from Tankyrase-mediated protein destruction, which results in its stabilization and subsequent hyperactivation of the SRC, SYK and VAV signalling pathways.

Introduction

Cherubism is a dominantly inherited disorder characterized by facial disfigurement, early tooth loss, failure of permanent tooth eruption and distortion of the orbital socket creating an upturned eye appearance occasionally associated with blindness (Jones *et al.*, 1950). Interosseous fibrocystic lesions arise in cherubism patients as a result of highly activated

Correspondence: Robert, Rottapel@uhnres.utoronto.ca, 416-581-7852.
*These authors contributed equally to the work

osteoclasts and infiltrating inflammatory and mesenchymal cells. The cherubism locus was mapped to chromosome 4p16 (Tiziani et al., 1999) with subsequent identification of single missense mutations in the gene encoding the adapter protein 3BP2 within this locus (Ueki *et al.*, 2001). 3BP2 contains an N-terminal pleckstrin homology (PH) domain, a proline-rich stretch that binds to Src homology (SH)-3 domain containing proteins, and a C-terminal SH2 domain that binds to phosphotyrosine residues (Deckert, 2006) (Figure 1D). Most 3BP2 mutations associated with cherubism cluster within a peptide sequence RSPPDG lying between the PH and SH2 domains. A mouse model of cherubism in which the most common disease-associated allele, P416R was knocked-in to the *Sh3bp2* locus, develop severe osteoporosis associated with highly activated osteoclasts and demonstrated that mutation within this peptide sequence results in a gain-of-function phenotype (Ueki *et al.*, 2007). Analysis of mice harbouring two copies of the cherubism allele uncovered 3BP2 as a major governor of myelomonocytic homeostatic cell numbers. Homozygous mice die of a systemic inflammation disorder at 25 weeks of age as a result of myelomonocytic infiltration of the skin, synovial lining, and visceral organs associated with elevated serum TNFα levels, trabecular bone loss and cortical bone erosions (Ueki et al., 2007).

3BP2 was originally identified as a binding protein of the tyrosine kinase ABL SH3 domain through proline-rich sequences lying between the PH and SH2 domain (Cicchetti *et al.*, 1992). 3BP2 is part of a multiprotein signalling complex composed of the SRC family kinases (SFKs), SYK and the RHO family guanine nucleotide exchange factor VAV (Deckert and Rottapel, 2006) and is required for optimal B cell antigen receptor (Chen et al., 2007; de la Fuente et al., 2006) and integrin activation (Levaot et al., 2011). The biochemical basis by which cherubism mutations alter the activity of the 3BP2 adapter protein has remained elusive. The tight cluster of mutations in the peptide sequence of 3BP2 observed in cherubism patients suggested to us that this sequence might define a protein interaction motif.

Here we identify the poly(ADP-ribose)polymerase (PARP) family member Tankyrase as the protein which binds to the RSPPDG sequence and serves to repress 3BP2 protein levels through ADP-ribosylation and subsequent ubiquitylation by the E3-ubiquitin ligase RNF146. We demonstrate that cherubism mutations disrupt 3BP2 binding to Tankyrase and stabilize the 3BP2 protein. Our accompanying manuscript provides the structural basis of 3BP2 peptide recognition by the ankyrin repeats of Tankyrase, a mechanism shared by all known Tankyrase substrates. The structural insights enable us to rationalize how cherubism mutations allow 3BP2 to escape recruitment by Tankyrase. Elevated steady state protein levels of 3BP2 observed in primary osteoclasts derived from cherubism mutant mice are associated with high levels of SRC, SYK and VAV activity while osteoclasts lacking 3BP2 are unable to normally activate SRC, SYK and VAV. Lastly, we show that inhibition of Tankyrase in osteoclasts *in vitro* or depletion of Tankyrase *in vivo* recapitulates many of the phenotypic features of cherubism. These genetic and pharmacologic experiments provide direct evidence that Tankyrase is a negative regulator of the SRC signalling pathway through its action on 3BP2. Our study elucidates the biochemical basis underlying the pathogenesis of cherubism and uncovers Tankyrase as a previously unknown component of a regulatory pathway controlling bone homeostasis and inflammatory cytokine production.

Results

Cherubism mutations increase 3BP2 protein stability

We examined the levels of 3BP2 protein expressed in osteoclast progenitors, primary bone marrow-derived macrophages from wild type mice (Figure 1A, lanes 1 and 2) or mice harbouring one ($Sh3bp2^{KI/+}$) (Figure 1A, lanes 3 and 4) or two alleles ($Sh3bp2^{KI/KI}$) (Figure 1A, lanes 5 and 6) of the cherubism mutation P416R. Strikingly, the steady-state level of

3BP2 was increased in macrophages derived from both the hetero- and homozygote cherubism mutant mice. Quantitative PCR indicated that the levels of *sh3bp2* mRNA in macrophages were similar between the three different mice strains (Figure 1B). This observation raised the possibility that cherubism arises as a result of a gain-of-function mutation leading to the accumulation of 3BP2 protein. To determine if the cherubism mutation altered the stability of 3BP2 we performed a cycloheximide chase experiment on wild type- or *Sh3bp2*$^{KI/KI}$–derived bone marrow macrophages. As shown in Figure 1C, the half-life of the wild type 3BP2 protein was 6.5 h compared to 31.4 h for the cherubism mutant form of the protein. These data demonstrate that the P416R cherubism mutation increases the protein stability of 3BP2.

3BP2 binds to Tankyrase, an interaction disrupted by cherubism mutations

We conjectured that the 3BP2-**RSPPDG** sequence might define a docking site for a negative regulatory protein responsible for controlling 3BP2 protein levels, which is uncoupled by the cherubism mutations. We used the yeast two-hybrid system with full-length 3BP2 as bait to identify 3BP2-binding proteins from a hematopoietic cell library. From this screen we identified Tankyrase-2 (TNKS2) as a potential 3BP2 interacting protein. TNKS2 is a member of the poly(ADP-ribose)polymerase (PARP) family of proteins, which catalyze the addition of ADP-ribose from NAD^+ to acceptor proteins. TNKS2 is most closely related to Tankyrase 1 (TNKS), a protein originally identified as a repressor of the telomerase inhibitor TRF1/TERF1 (Smith et al., 1998). TNKS and TNKS2 contain five ankyrin repeat clusters (ARCs, see accompanying manuscript), a sterile alpha motif (SAM) domain mediating multimerization and the PARP catalytic domain (Figure 1D).

We showed that epitope-tagged versions of both TNKS and TNKS2 bind to 3BP2 in transfected HEK293T cells (Figure 1E). We next tested the capacity of 3BP2 proteins harbouring any one of three independent cherubism mutations within the RSPPDG motif R413Q, P416H or G418R, to bind to TNKS2 and showed that none of the cherubism mutants were able to bind to TNKS2 (Figure 1F, lane 5–7). In contrast, a mutant form of 3BP2 which contains a mutation in its SH2 domain (R486K) rendering it unable to bind to phosphotyrosine-containing proteins (Sada et al., 2002), bound to TNKS2 comparably to the wild type protein (Figure 1F, lane 4). These data demonstrate that the cherubism mutations disrupt binding between 3BP2 and TNKS2.

A recombinant GST-fusion protein containing the 3BP2 RSPPDG six amino acid sequence (GST-Hex) immobilized on glutathione-sepharose was sufficient to recruit TNKS2 from HEK293T cell lysates (Figure 1G, lane 5) but not resin alone or resin coupled to GST (Figure 1G, lanes 3 and 4). However, GST-Hex peptides containing any of the three cherubism mutations failed to interact with TNKS2 (Figure 1G, lanes 6–8). These data and those presented in Figure 1F show that the RSPPDG sequence in 3BP2 mutated in cherubism patients is both necessary and sufficient to mediate binding with TNKS2.

We mapped the interaction between 3BP2 and TNKS2 by deletion mutagenesis. TNKS2 constructs lacking either the first or the second half of the ankyrin region bound to 3BP2, whereas binding was lost when the entire ankyrin region was deleted (Figure S1). This suggests that 3BP2 likely binds to more than one of the ARCs in TNKS2 as confirmed in our accompanying manuscript. The interaction between 3BP2 and TNKS2 was not dependent on the SAM domain (Figure S1). Using fluorescence polarization, we quantified binding between the recombinant N-terminal region of TNKS2 containing all five ARCs and the 3BP2 Tankyrase targeting peptide and determined a dissociation constant of 0.5 ± 0.1 μM (see accompanying manuscript).

Wild type 3BP2 but not 3BP2 cherubism mutants are ribosylated by Tankyrase

To determine if 3BP2 is a TNKS2 substrate, we performed an *in vitro* ribosylation assay. Radioactive [^{32}P]NAD^{+} was added as a source of ADP-ribose to 3BP2 immune complexes precipitated from HEK293T cells over-expressing TNKS2 and 3BP2. The reaction was resolved by SDS-PAGE and revealed by autoradiography. We observed two bands corresponding to the size of 3BP2 (~80 kDa) and TNKS2 (~120 kDa) respectively, or a yet to be identified co-purifying protein (Figure 2A, lane 2). Ribosylation was much stronger for the higher molecular weight species compared to the lower molecular weight protein and was dependent on an intact TNKS2 SAM and PARP domain (Figure 2A, lanes 3 and 4). Addition of the PARP inhibitor PJ-34 (10μM) at a concentration above the IC50 for Tankyrase was sufficient to inhibit ribosylation of both the lower- and higher-molecular-weight ribosylated species (Figure 2B, lane 3).

To determine the effect of the cherubism mutation on 3BP2 ribosylation, we subjected three mutant forms of 3BP2, R413Q, P416H, or G418R, derived from cherubism patients to an *in vitro* ribosylation assay. Whereas wild type 3BP2 and TNKS2 formed a complex and were ribosylated (Figure 2C, lane 3), none of the three cherubism mutants bound to TNKS2 nor became ribosylated (Figure 2C, lanes 4–6) suggesting that the biochemical defect observed in cherubism may result from the failure of 3BP2 to bind to TNKS2 and be modified by ADP-ribose conjugation.

To confirm the identity of the ribosylated 120 kDa species present in 3BP2 immune complexes, we dissociated proteins in 1% heated SDS, re-precipitated TNKS2 and probed the immunoprecipitates with either an antibody that recognizes ADP-ribose (PAR) or an anti-TNKS2 antibody. We confirmed that TNKS2 is autoribosylated in 3BP2 immune complexes (Figure 2D, lane 3) but not in cherubism mutant 3BP2 protein complexes (Figure 2D, lanes 4–6).

We next sought to determine if endogenous 3BP2 is ribosylated in primary osteoclasts. 3BP2 immune complexes derived from wild type or *Sh3bp2*$^{KI/KI}$ osteoclasts were probed with the anti-PAR antibody. We observed that endogenous 3BP2 was ribosylated, and was associated with an abundantly ribosylated protein with a molecular weight similar to TNKS2 and high molecular weight ribosylated species of unknown identity. Ribosylation was dramatically reduced in 3BP2 protein complexes derived from osteoclasts obtained from cherubism mice (Figure 2E). Again we noticed that the level of 3BP2 protein present in the *Sh3bp2*$^{KI/KI}$ -derived osteoclasts was significantly elevated compared to the wild type controls (Figure 2E, row 2). We showed that an N-terminal fragment of 3BP2 containing the **RSPPDG** sequence and a C-terminal fragment beginning with the **RSPPDG** sequence were both ribosylated by Tankyrase, showing that 3BP2 is either modified at multiple sites through out the protein or that a single ribosylation site lies in the 13 amino acid stretch common to both constructs (Figure S2A).

Although we found that the Tankyrase-binding sequence in 3BP2 is sufficient for the recruitment of Tankyrase (see above), it remained possible that its position in 3BP2 contributes to Tankyrase recruitment and/or ribosylation. To determine the positional effects of the Tankyrase-binding sequence on 3BP2 stability and ribosylation, we created a chimeric protein in which the non-mutated RSPPDG sequence was added to the C-terminus of the cherubism mutant 3BP2R413Q. Tankyrase was able to bind to the chimeric protein but was unable to alter the steady state levels of the chimeric protein **or** induce ribosylation (Figure S2B-D). These data suggest that 3BP2 ribosylation and destabilization are sensitive to the position of the Tankyrase-binding sequence in 3BP2.

Ribosylation of the wild type but not a cherubism mutant form of 3BP2 by TNKS2 induces 3BP2 ubiquitylation and subsequent degradation

We investigated whether TNKS2 could directly regulate 3BP2 protein levels. Wild type 3BP2 or the cherubism mutant 3BP2R413Q was co-expressed with increasing amounts of the TNKS2 expression vector. We observed that while the steady-state level of 3BP2 was inversely related to TNKS2 protein level, the 3BP2R413Q mutant was resistant to the effects of TNKS2 over-expression (Figure S3A). To determine if the PARP domain was required for TNKS2-induced 3BP2 destabilization, we repeated the experiment with a PARP domain deleted mutant form of TNKS2. While TNKS2ΔPARP and 3BP2 formed a complex (see Figure S3B, row 3), 3BP2 protein levels were unaffected by increasing levels of TNKS2ΔPARP (Figure S3B). These data show that the ability of TNKS2 to perturb 3BP2 protein levels is not a result of binding alone but requires the intact TNKS2 catalytic domain.

We sought to elucidate the mechanism underlying the regulation of 3BP2 protein stability by TNKS2. Conceivably, TNKS2-mediated ribosylation could mark 3BP2 for ubiquitylation and subsequent proteasome-mediated degradation. To test this possibility, we co-expressed 3BP2 and TNKS2 in the absence or presence of proteasome inhibitors. We observed that the diminished steady-state levels of 3BP2 resulting from co-expression of TNKS2 was reversed in the presence of proteasome inhibitors (Figure 3A). We noticed that TNKS2 levels were diminished when co-expressed with wild type 3BP2 but not cherubism mutants (Figure 1E, 1F, 2C, and 2D) suggesting that both components of the complex are rendered unstable by the interaction and stabilized by proteasome inhibition. We sought to determine whether endogenous 3BP2 was ubiquitylated in response to TNKS2 expression. A tagged version of ubiquitin was expressed in cells in the presence or absence of ectopically expressed TNKS2. Endogenous 3BP2 was then immunoprecipitated and probed for ubiquitin modification by Western blotting. Whereas little ubiquitin was detected in 3BP2 immunoprecipitates in the absence of TNKS2, intense ubiquitylation of proteins present in the 3BP2 complex, seen as a diffuse smear, was induced when TNKS2 was co-expressed (Figure 3B, lane 2 vs. lane 4).

To determine whether TNKS2 PARP activity was required to stimulate 3BP2 ubiquitylation, we repeated the experiment in the presence of the non-selective PARP inhibitor PJ-34 and observed that the TNKS2 induction of 3BP2 ubiquitylation was blocked (Figure 3B, lane 5 and 6). We confirmed that 3BP2 is itself ubiquitylated, by a precipitation-reprecipitation experiment under denaturing conditions (Figure S3C). These data show that endogenous 3BP2 ubiquitylation is stimulated by TNKS2 and requires PARP activity.

To ascertain the form of TNKS2-dependent ubiquitin modification of 3BP2, we used a monoclonal antibody, which recognizes lysine 48 (Ub-K48) and observed that TNKS2 induced intense step-wise K48 ubiquitin modification of likely to be 3BP2 (Figure 3C, lane 2). To determine the effect of the cherubism mutation on 3BP2 ubiquitylation we expressed wild type 3BP2 or the cherubism mutant 3BP2R413Q in the absence or presence of TNKS2. Whereas wild type 3BP2 became polyubiquitylated in the presence of TNKS2, the 3BP2 cherubism mutant poorly incorporated ubiquitin (Figure 3C, lanes 3 and 4).

The E-3 ubiquitin ligase RNF146 has recently been shown to regulate the Tankyrase dependent ubiquitylation of Axin2 (Zhang et al., 2011). RNF146 may be widely employed as an ubiquitin ligase for additional Tankyrase substrates, and we tested whether RNF146 also targets ribosylated 3BP2. We showed that RNF146 binds to 3BP2 but not to a cherubism mutant or to wild type 3BP2 in cells in which Tankyrase PARP activity has been inhibited by the Tankyrase selective inhibitor XAV939 (Figure 3D and E). Importantly, co-expression of RNF146 abolished the detection of the 3BP2:Tankyrase complex suggesting that RNF146 might be part of a destruction complex involving 3BP2 and Tankyrase (Figure

3D and E, 2nd row). Moreover, wild type RNF146, but not a mutant form of the ligase lacking its ring finger or the WWE ADP-ribose binding domain, potently stimulated K48 ubiquitylation of 3BP2 (Figure 3F). Depletion of RNF146 in HEK293T cells by three independent interfering RNA hairpin lentiviruses, which efficiently knocked down RNF146 transcript resulted in increased steady-state levels of 3BP2 (Figure 3G and S3D) demonstrating that RNF146 is the functional E3-ligase controlling 3BP2 protein levels.

Elevated levels of wild type 3BP2 protein are sufficient to induce enhanced osteoclast formation and TNFα secretion by macrophages

Our data demonstrate that cherubism mutations result in the stabilization of 3BP2 protein as a result of loss of repression by Tankyrase. We next asked whether the cherubism-associated characteristics of an *in vitro* culture of osteoclasts result from elevated 3BP2 levels or from some other neomorphic changes associated with these mutations. We over-expressed wild type 3BP2 or the cherubism mutant allele P416R at similar levels using retroviral transduction in the RAW264.7 monocytic cell line, which have osteoclastogenic potential (Figure 4A). We observed that over-expression of either wild type 3BP2 or the 3BP2P416R cherubism mutant induced the formation of multinucleated Tartrate-resistant acid phosphatase (TRAP) positive cells in the absence of RANKL while no multinucleated cells were observed in empty vector-transduced control cells (Figure 4B). Moreover, RAW264.7 cells ectopically expressing either wild type or a cherubism mutant variant of 3BP2 secreted high levels of TNFα compared to vector-infected controls (Figure 4C). These results demonstrate that elevated levels of wild type 3BP2 protein are sufficient to induce enhanced osteoclast formation in the absence of RANKL and increased TNFα secretion by macrophages consistent with the idea that the basis of cherubsim results from elevated levels of 3BP2 and not due to a neomorphic protein property of the protein.

Enhanced activation of SRC, SYK and VAV in cherubism osteoclasts

3BP2 nucleates a signalling complex that contains SRC kinases, SYK and the guanine nucleotide exchange factor VAV (Deckert and Rottapel, 2006). To understand the effect of 3BP2 stabilization on the signalling pathways which 3BP2 connects to, we examined the phosphorylation levels of SRC, SYK and VAV as a surrogate of their activation state. SRC, SYK and VAV were highly tyrosine-phosphorylated in osteoclasts derived from *Sh3bp2*$^{KI/KI}$ mice compared to osteoclasts from control mice, while total SYK, SRC and VAV protein levels were similar in osteoclasts derived from both mouse strains (Figure 4D). To verify that the activities of SRC and SYK were elevated we performed *in vitro* kinase assays on both proteins. Both SRC (Figure 4E) and SYK (Figure 4F) autophosphorylation levels were elevated in cherubism osteoclasts compared to normal controls. Similarly, the increased levels of VAV phosphorylation correlated with elevated levels of RAC-GTP in the osteoclasts from cherubism mice as measured by a PAK-CRIB RAC binding pull down assay (Figure 4G, lanes 3 and 6)).

TNKS/TNKS2 depleted osteoclasts phenocopy cherubism osteoclasts

To test whether the failure of TNKS2-mediated negative regulation of 3BP2 observed in cherubism osteoclasts accounted for their activated phenotype, we examined whether TNKS2 deficient osteoclasts phenocopied cherubism osteoclasts. Wild type macrophages normally complete osteoclastogenesis *in vitro* within five to six days when cultured in RANKL and CSF-1. We cultured bone marrow monocytes (BMMs) from wild type or *Tnks2*$^{-/-}$ mice in the presence of increasing doses of RANKL for the suboptimal period of three days and observed an enhanced rate of *in vitro* osteoclastogenesis intermediate between wild type and *Sh3bp2*$^{KI/KI}$ macrophages (Figure 5A, rows 1–3). Since TNKS and TNKS2 have overlapping essential function during embryonic development (Chiang et al., 2008) we conjectured that TNKS may also participate in 3BP2 negative regulation in

osteoclasts. We observed that both *tnks* and *tnks2* mRNAs are expressed during osteoclast differentiation (Figure 5B) and demonstrated that TNKS can bind to and PARsylate 3BP2 when co-expressed in HEK293T cells (Figure 1E and S4A). We therefore depleted *tnks* mRNA in the $Tnks2^{-/-}$ BMMs using a lentivirus shRNA specific for *tnks* (Figure 5C) and observed that BMMs lacking both TNKS and TNKS2 underwent accelerated osteoclastogenesis closely resembling the activated osteoclast phenotype observed in cherubism osteoclasts (Figure 5A, row 4). Moreover, we noted that in TNKS/TNKS2 depleted cells, SRC, SYK and VAV were highly phosphorylated and 3BP2 levels were elevated (Figure 5D, lane 4 and 5E, lane 4, row 4). These results were observed with a second *tnks*-depleting hairpin lentivirus (data not shown). These data demonstrate that both Tankyrase family proteins participate in the repression of 3BP2 protein levels and the control of SRC, SYK and VAV activation in macrophages and osteoclasts. Lastly, we observed that wild type macrophages depleted of RNF146 similarly underwent accelerated osteoclastogenesis with elevated 3BP2 levels reminiscent of the $Sh3bp2^{KI/KI}$ or Tankyrase-depleted macrophages (Figure 5F, G and S4B). This effect was dependent on 3BP2 as RNF146 depletion in 3BP2 knock out cells had little effect on *in vitro* osteoclastogenesis. RNF146 therefore controls osteoclast activity by regulating 3BP2 levels in an ADP-ribose dependent manner.

Tankyrase inhibition promotes osteoclastogenesis and TNFα secretion by macrophages

To determine if the activated osteoclast phenotype observed in cells depleted of TNKS/TNKS2 was dependent on 3BP2, we applied the non-selective PARP inhibitor PJ-34 or the recently described TNKS/TNKS2 specific inhibitor IWR-1 (Chen et al., 2009; Huang et al., 2009) to either wild type or 3BP2-deficient BMMs cultured under osteoclastogenic conditions. Exposure of wild type BMMs to either PJ-34 or IWR-1 resulted in acceleration of osteoclast formation compared to untreated control cells (Figure 6A, top row). 3BP2-deficient BMMs, however were completely resistant to the pro-osteoclast effects of either inhibitor (Figure 6A, bottom row) demonstrating that 3BP2 is the relevant Tankyrase target in these inhibition studies. Osteoclasts treated with either PJ-34 or IWR-1 exhibited increased levels of phosphorylated SRC, SYK and VAV and elevated levels of 3BP2 protein compared to control cells (Figure 6B, lanes 1–3, 6C, row 4 lanes 1–3). Moreover, SRC, SYK and VAV failed to become phosphorylated in cells lacking 3BP2 treated with PARP inhibitors (Figure 6B, lanes 4–6) demonstrating that 3BP2 is an obligate factor required for SRC pathway activation in osteoclasts differentiation. We next tested the effect of Tankyrase inhibition on basal TNFα production in macrophages. We observed that wild type macrophages treated with CSF-1 and IWR-1 for 36 hours secreted 2 fold higher levels of TNFα compared with vehicle controls (Figure 6D) and at levels similar to $Sh3bp2^{KI/KI}$-derived macrophages, while there was no induction of TNFα observed in treated $Sh3bp2^{-/-}$-derived macrophages. These data provide conclusive evidence that TNKS/TNKS2 negatively regulate the activation of SRC and its downstream targets SYK and VAV in osteoclasts by controlling the abundance of 3BP2. Moreover, genetic depletion or pharmacologic inhibition of Tankyase resulted in an increased response of myeloid cells to CSF-1, an effect phenocopied by the $Sh3bp2^{KI/KI}$-derived monocytes.

To test whether SRC activity is required for Tankyrase- and 3BP2-mediated osteoclast differentiation, we applied the SRC inhibitors AZD0530 or PP1 to wild type or $Sh3bp2^{KI/KI}$ derived macrophages under osteoclastogenic conditions. Incubation with either inhibitor blocked osteoclast formation of both wild type and $Sh3bp2^{KI/KI}$–derived BMMs (Figure 6E). Moreover, addition of these SRC inhibitors to wild type BMM cultures treated with the PARP inhibitor IWR-1 similarly blocked osteoclast formation (Figure 6F). Taken together, the results demonstrate that SRC is required as a downstream effector of the

Tankyrase-3BP2 signalling module and that hyperactivation of osteoclasts mediated by stabilized 3BP2 can be antagonized by SRC inhibition.

Radiation chimeric mice that lack TNKS/TNKS2 copy the phenotype of *Sh3bp2*$^{KI/KI}$ mice

Our observations suggest that Tankyrase proteins may have a physiologic role in regulating bone homeostasis, myelomonocytic expansion and in controlling inflammatory cytokines as observed in the *Sh3bp2*$^{KI/KI}$ mice. We predicted that mice lacking Tankyrases within the bone marrow compartment would recapitulate these features of the cherubism mice. We analyzed the trabecular bone volume and serum TNFα levels of 22 weeks old *Tnks2*$^{-/-}$ mice and observed no difference in these parameters compared to age-matched wild type littermate controls (Figure S5A-C). The failure of *Tnks2*$^{-/-}$ mice to show a cherubism-like phenotype could be the result of the redundant function of TNKS in the hematopoietic compartment. To test whether loss of both TNKS and TNKS2 in the hematopoietc system could recapitulate the cherubism phenotype, we created chimeric mice in which TNKS was knocked down in the *Tnks2*$^{-/-}$ background. We depleted TNKS by RNAi-mediated knock down with a lentivirus harbouring a *Tnks*-specific shRNA in lineage-depleted *Tnks2*$^{-/-}$ bone marrow cells (C57Bl/6, CD45.2). Infected bone marrow cells were then injected into lethally irradiated, syngeneic (CD45.1) recipient mice. Wild type transplantation control chimeric mice were generated from CD45.2-derived bone marrow cells infected with a lentivirus expressing a scrambled shRNA hairpin (Figure 7A). Fifteen weeks following transplantation, we evaluated engraftment by measuring the percentage of CD45.2 positive leukocytes in the peripheral blood. Both wild type-control and TNKS/TNKS2-depleted bone marrow engrafted at similar levels of 38% of peripheral blood leukocytes (Figure 7B). TNKS/TNKS2-deficient chimeras showed a trend towards expansion of the CD11b-positive myelomonocytic cells compared to wild type chimeras (30% versus 14%, of blood leukocytes, respectively, p=0.16) (Figure 7C) suggesting that TNKS/TNKS2 are required to restrain expansion of the myelomonocytic lineage. We then analyzed the trabecular bone volume/total bone volume ratio (BV/TV) of the chimeric mice from each group by micro-computer tomography (μCT). Relative to the wild type chimeric mice we observed that the TNKS/TNKS2 chimeric mice had a dramatic reduction in trabecular bone volume of 33% (Figure 7D). TRAP staining of tibias of TNKS/TNKS2-deficient chimeras showed a profound increase in TRAP positive cells compared to wild type chimeras (red stain, Figure 7E). Histomorphometric analysis showed a two-fold increase in the ratio of osteoclast surface to total bone surface and 70% increase in osteoclast number per bone surface in TNKS/TNKS2-deficient chimeras (Figure 7F and G). We next examined the *in vitro* culture properties of osteoclasts from both sets of chimeric mice and observed enhanced osteoclastogenesis of BMMSs derived from TNKS/TNKS2 chimeric mice, characteristic of the cherubism phenotype (Figure 7H). These data provide strong genetic evidence that ablation of TNKS/TNKS2 *in vivo* phenocopies the hallmark features of bone loss and activated osteoclasts characteristic of cherubism.

Discussion

In this study, we uncover an enzyme-substrate relationship between the poly(ADP-ribose)polymerase Tankyrase and 3BP2, a signalling adapter protein upstream of SRC kinases, which is mutated in cherubism. Tankyrase-mediated poly(ADP-ribosyl)ation promotes 3BP2 turnover by targeting it to the ubiquitin-proteasome machinery. We show that mutations that give rise to cherubism stabilize 3BP2 and thereby increase its signalling potential to drive osteoclast differentiation characteristic of the cellular dysfunction underlying cherubism. We examined whether cherubism mutations might confer neomorphic properties to 3BP2 that are responsible for the cherubism phenotype. We observed that overexpression of the wild type 3BP2 protein was sufficient to induce

osteoclast formation (even in the absence of RANKL) and elevated TNFα secretion in macrophages, two critical features of the cherubism phenotype. These data argue that stabilization of 3BP2 protein is the basis for the hypermorphic behaviour of cherubism variants of 3BP2 and provide an explanation for the autosomal dominant inheritance of the disease. The ability of over-expressed 3BP2 to manifest cherubism-like effects is therefore not likely due to a neomorphic property of the protein resulting from these mutations, but rather is due to the intrinsic accentuated property of the wild type 3BP2 protein. Cherubism mutations reside within a Tankyrase-recruiting peptide motif in 3BP2 and abolish recognition of 3BP2 by Tankyrase. In an accompanying manuscript, we provide a crystal structure of the 3BP2 peptide bound to a TNKS2 ankyrin repeat and determine the general rules for substrate recognition by Tankyrase. It is important to note that all of the known cherubism mutations described to date (Lietman et al., 2006) violate these rules providing further evidence for the role of disrupted Tankyrase binding as the cause of cherubism. We have highlighted the importance of this interaction by showing that interference with Tankyrase expression or activity *in vitro* similarly leads to enhanced 3BP2 expression and to hyperactivated osteoclasts and increased TNFα production by monocytes. Lastly, we have shown that the characteristic cherubism features of bone loss, increased numbers of *in situ* TRAP positive osteoclasts and myelomonocytic expansion can be recapitulated *in vivo* in TNKS/TNKS2 deficient bone marrow chimeric mice.

These studies have highlighted that 3BP2 is a concentration-limited factor required for SRC activation in osteoclasts and that modulation of the steady state levels of 3BP2 tightly control SRC activity and downstream signalling proteins in these cells. We demonstrated that SRC inhibition blocked osteoclastogenesis associated with cherubism or Tankyrase-inhibited BMMs suggesting that SRC lies downstream of 3BP2 or is a generally required component for osteoclast formation. These studies also suggest that therapeutic use of SRC kinase inhibitors might benefit cherubism patients.

The biologic function of the Tankyrase proteins is complicated by the multiplicity of identified binding proteins. Mice lacking TNKS or TNKS2 develop normally through embryogenesis. However, adult *Tnks*$^{-/-}$ mice suffer from a metabolic disorder (Yeh et al., 2009) while *Tnks2*$^{-/-}$ mice have a short stature phenotype (Chiang et al., 2006; Hsiao et al., 2006). Mice lacking both TNKS and TNKS2 die *in utero* at post coital day 10 demonstrating that Tankyrase proteins have an essential but redundant function during embryonic development (Chiang et al., 2008). TNKS was originally identified as a negative regulator of the telomerase inhibitor TRF1/TERF1 (Smith et al., 1998). TRF1/TERF1 is similarly regulated by ADP-ribosylation and ubiquitin-mediated proteolysis (Chang et al., 2003). More recently, Tankyrases have been identified as a positive regulator of the Wnt/β-catenin pathway through their capacity to negatively regulate AXIN through ADP-ribosylation and ubiquitylation (Huang et al., 2009). Both TNKS and TNKS2 bind to the mitotic spindle regulator NUMA, but TNKS alone is required for NUMA ribosylation and proper mitotic spindle organization (Chang et al., 2005). TNKS and TNKS2 bind to a common set of proteins including insulin responsive amino peptidase (IRAP), TAB182, and FBP17 all of whom share a common RXXPDG binding motif that is similar to the 3BP2 Tankyrase binding peptide sequence mutated in cherubism. In the accompanying manuscript we identify sequence rules for tight binding of targeting peptides by Tankyrase, which may facilitate the identification of previously unknown Tankyrase substrates.

Tankyrase inhibition has been proposed as a strategy to treat Wnt-dependent tumors (Huang et al., 2009). However, the established role for SRC in controlling osteoclast and macrophage function (Boyce et al., 1992), in addition to its role in potentiating tumorigenesis suggests that sustained pharmacologic inhibition of Tankyrase proteins might lead to the untoward effects of osteoporosis, myelomonocytic-mediated inflammation or

tumor promotion. Our studies also raise the possibility that high expression of 3BP2 or loss-of-function of Tankyrase may contribute to highly active SRC observed in a some human cancers (Du et al., 2009; Hynes, 2000; Irby and Yeatman, 2000; Talamonti et al., 1993; Wiener et al., 2003).

We investigated the manner in which 3BP2 ribosylation is coupled to ubiquitylation. Several distinct PAR-binding motifs have recently been described including the PAR-binding macro domain (Karras et al., 2005) a short amino acid sequence rich in basic and hydrophobic residues capable of PAR recognition found in p53, histones and XRCC1 (Gagne et al., 2003; Pleschke et al., 2000) and a poly(ADP-ribose)-binding zinc finger (PBZ) motif present in Aprataxin PNK-like factor (APLF) involved in DNA damage response and Checkpoint Protein with FHA and RING domains (CHFR) a ubiquitin ligase involved mitotic checkpoint control in response to microtubule poisons (Ahel et al., 2008). Recently RNF146 has been shown to mediate the ubiquitylation of Axin2 in a ADP-ribose dependent fashion (Zhang et al., 2011). We show here that RNF146 binds to 3BP2 but not to cherubism mutants and that binding is dependent on Tankyrase activity. We show that depletion of RNF146 results in the accumulation of 3BP2 and provokes accelerated osteoclastogenesis in a manner observed in cherubism osteoclasts or in osteoclasts lacking Tankyrase proteins. These data identify the E3 ligase RNF146 as a 3BP2-dependent regulator of osteoclast activity. It appears increasingly likely that RNF146 generally recognizes ribosylated Tankyrase substrates.

We have identified ADP-ribosylation as a regulatory switch that controls 3BP2 protein levels as a mechanism to modulate SRC kinase activity and downstream signalling molecules in osteoclasts. The necessity to maintain strict control of the 3BP2/SRC signalling module is underscored in homozygous cherubism mutations in mice, where uncoupling of 3BP2 from Tankyrase-mediated negative regulation results in lethality as a result of systemic myelomonocytic cell infiltration into skin and visceral organs. We have demonstrated that loss of this regulatory pathway is the basis of the molecular mechanism underlying cherubism pathogenesis. Cherubism thus represents an example of a human developmental disease resulting from a defect in ADP-ribosylation.

Experimental Procedures

Mice

Sh3bp2$^{KI/KI}$ mice were a kind gift from Dr. Bjorn Olsen (Harvard School of Medicine, Boston). Derivation of *Sh3bp2*$^{-/-}$ mice has been previously described (Chen et al., 2007). *Tnks2*$^{-/-}$ mice were a kind gift from Dr Richard Hodes (National Institutes of Health, Bethesda).

Chimeric mice

Bone marrow cells from wild type or *Tnks2*$^{-/-}$ mice (CD45.2) were lineage depleted. 10^6 lineage-depleted wild type or *Tnks2*$^{-/-}$ bone marrow cells were infected with pLKOTRC 020 lentivirus (TRC consortium, Broad Institute), and then injected together with 10^5 CD45.1 recipient bone marrow cells into the tail vein of eight-week-old irradiated (9Gy) B6.SJL recipient mice. Percent chimerism was evaluated by flow cytometry for the percent CD45.2$^+$ lymphocytes in the peripheral blood. For details see extended experimental procedures.

Microcomputed tomography

μCT (SkyScan) was performed on tibias of chimeric mice 15 weeks after injection. For details see extended experimental procedures.

Bone marrow cultures

Nucleated bone marrow cells were purified from mice femora and tibia. Osteoclast differentiation was induced by culturing non-adherent cells in the presence of RANKL and CSF-1. Tartrate-resistant acid phosphatase (TRAP) staining was performed using the Sigma reagent (386A) according to manufacturer protocol. For experiments with BM-derived macrophages, non-adherent cells were cultured for 3 days in the presence of CSF-1. For details see extended experimental procedures.

TNFα ELISA

TNFα in cultured medium was measured using a TNFα ELISA kit (eBioscience) according to the manufacturer protocol.

Retroviral transduction

BMMs were infected with PLKO.1 for 48 h in the presence of 8 μg/ml polybrene (Sigma). Infected cells were selected in puromycin (1.6μg/ml) for 3 days and then replated for osteoclast differentiation assay. For details see extended experimental procedures.

GST fusion peptide construction and binding assay

GST fusion peptides encompassing either wild type or cherubism mutant residues 413–418 of 3BP2 were purified and eluted from glutathione sepharose beads using standard procedures. HEK293T cells expressing Flag-TNKS2 were lysed and recombinant GST-3BP2 wild type or cherubism peptide fusion proteins were added to the lysates. Tankyrase binding to the GST-3BP2 peptides was then determined by Western blot. For details see extended experimental procedures.

Immunoprecipitation and Western blotting

Transfected cells were lysed, pre-cleared with protein A/G-sepharose, then the lysates were incubated with the indicated antibody. For reprecipitation experiments, immune complexes were dissociated in heated 1% SDS buffer cooled and then incubated in 20 mM iodoacetamide prior to dilution with 1 ml of lysis buffer and addition of the secondary antibody for reprecipitation. See extended experimental procedures.

In vitro PARP assay

TNKS2, 3BP2 wild type or cherubism mutants were transiently expressed in HEK293T cells for 48 h and then cells were lysed. 3BP2 immune complexes were washed in 100 μl of PARP reaction buffer (50 mM Tris.HCl, pH 8.0, 4 mM $MgCl_2$, 0.2 mM dithiothreitol) and incubated in 100 μl of PARP reaction buffer containing 25 μCi of [^{32}P]NAD^+ (1000 Ci/mmol; GE Healthcare) for 30 min at 25°C. Following completion of the PARP reaction, beads were washed and proteins resuspended in sample buffer, fractionated by SDS-PAGE and the gels dried prior to detection by autoradiography.

Statistical analysis

Data is presented as means ± Sem. Statistic significance was determined by Student's t test. P value < 0.05 was considered statistically significant.

Further detailed descriptions of the RAC-GTP pull down assay, *in vitro* kinase assay, reagents and antibodies and real-time PCRare in the extended experimental procedure s.

Supplementary Material

Refer to Web version on PubMed Central for supplementary material.

Acknowledgments

This work was supported by a grant from the Terry Fox Research Institute (TFPP Grant #20003), the Canadian Cancer Society Research Institute and by the Ontario Ministry of Health and Long Term Care. The views expressed do not necessarily reflect those of the OMOHLTC. R.R. is supported by the Amgen Chair for Cancer Research from the PMHF at the Ontario Cancer Institute, Princess Margaret Hospital. N.L. was supported by the Arthritis Centre for Excellence Fellowship, University of Toronto. Y.U. was supported by Charles H. Hood Foundation, Inc., Boston, MA and research grant R01DE020835 from the National Institutes of Health. We thank Gerald Gish for providing the peptides and Sebastian Geuttler for assistance with the fluorescence polarization experiments. We thank and Ben Neel and Norman Iscove for discussion regarding the chimera experiments. We thank Mauricio Medrano for graphic design. We thank Frank Sicheri, Sebastian Geuttler, Ernst Reichenberger, Gregg Morin, Vuk Stambolic, and Ben Neel for critical reading of the manuscript.

References

Ahel I, Ahel D, Matsusaka T, Clark AJ, Pines J, Boulton SJ, West SC. Poly(ADP-ribose)-binding zinc finger motifs in DNA repair/checkpoint proteins. Nature. 2008; 451:81–85. [PubMed: 18172500]

Boyce BF, Yoneda T, Lowe C, Soriano P, Mundy GR. Requirement of pp60c-src expression for osteoclasts to form ruffled borders and resorb bone in mice. J Clin Invest. 1992; 90:1622–1627. [PubMed: 1383278]

Chang P, Coughlin M, Mitchison TJ. Tankyrase-1 polymerization of poly(ADP-ribose) is required for spindle structure and function. Nat Cell Biol. 2005; 7:1133–1139. [PubMed: 16244666]

Chang W, Dynek JN, Smith S. TRF1 is degraded by ubiquitin-mediated proteolysis after release from telomeres. Genes Dev. 2003; 17:1328–1333. [PubMed: 12782650]

Chen B, Dodge ME, Tang W, Lu J, Ma Z, Fan CW, Wei S, Hao W, Kilgore J, Williams NS, et al. Small molecule-mediated disruption of Wnt-dependent signaling in tissue regeneration and cancer. Nat Chem Biol. 2009; 5:100–107. [PubMed: 19125156]

Chen G, Dimitriou ID, La Rose J, Ilangumaran S, Yeh WC, Doody G, Turner M, Gommerman J, Rottapel R. The 3BP2 adapter protein is required for optimal B-cell activation and thymus-independent type 2 humoral response. Mol Cell Biol. 2007; 27:3109–3122. [PubMed: 17283041]

Chiang YJ, Hsiao SJ, Yver D, Cushman SW, Tessarollo L, Smith S, Hodes RJ. Tankyrase 1 and tankyrase 2 are essential but redundant for mouse embryonic development. PLoS One. 2008; 3:e2639. [PubMed: 18612384]

Chiang YJ, Nguyen ML, Gurunathan S, Kaminker P, Tessarollo L, Campisi J, Hodes RJ. Generation and characterization of telomere length maintenance in tankyrase 2-deficient mice. Mol Cell Biol. 2006; 26:2037–2043. [PubMed: 16507984]

Cicchetti P, Mayer BJ, Thiel G, Baltimore D. Identification of a protein that binds to the SH3 region of Abl and is similar to Bcr and GAP-rho. Science. 1992; 257:803–806. [PubMed: 1379745]

de la Fuente MA, Kumar L, Lu B, Geha RS. 3BP2 deficiency impairs the response of B cells, but not T cells, to antigen receptor ligation. Mol Cell Biol. 2006; 26:5214–5225. [PubMed: 16809760]

Deckert M. The adaptor protein 3BP2 in leukocyte signaling. Med Sci (Paris). 2006; 22:1081–1086. [PubMed: 17156730]

Deckert M, Rottapel R. The adapter 3BP2: how it plugs into leukocyte signaling. Adv Exp Med Biol. 2006; 584:107–114. [PubMed: 16802602]

Du J, Bernasconi P, Clauser KR, Mani DR, Finn SP, Beroukhim R, Burns M, Julian B, Peng XP, Hieronymus H, et al. Bead-based profiling of tyrosine kinase phosphorylation identifies SRC as a potential target for glioblastoma therapy. Nat Biotechnol. 2009; 27:77–83. [PubMed: 19098899]

Gagne JP, Hunter JM, Labrecque B, Chabot B, Poirier GG. A proteomic approach to the identification of heterogeneous nuclear ribonucleoproteins as a new family of poly(ADP-ribose)-binding proteins. Biochem J. 2003; 371:331–340. [PubMed: 12517304]

Hsiao SJ, Poitras MF, Cook BD, Liu Y, Smith S. Tankyrase 2 poly(ADP-ribose) polymerase domain-deleted mice exhibit growth defects but have normal telomere length and capping. Mol Cell Biol. 2006; 26:2044–2054. [PubMed: 16507985]

Huang SM, Mishina YM, Liu S, Cheung A, Stegmeier F, Michaud GA, Charlat O, Wiellette E, Zhang Y, Wiessner S, et al. Tankyrase inhibition stabilizes axin and antagonizes Wnt signalling. Nature. 2009; 461:614–620. [PubMed: 19759537]

Hynes NE. Tyrosine kinase signalling in breast cancer. Breast Cancer Res. 2000; 2:154–157. [PubMed: 11250704]

Irby RB, Yeatman TJ. Role of Src expression and activation in human cancer. Oncogene. 2000; 19:5636–5642. [PubMed: 11114744]

Jones WA, Gerrie J, Pritchard J. Cherubism--familial fibrous dysplasia of the jaws. J Bone Joint Surg Br. 1950; 32-B:334–347. [PubMed: 14778852]

Karras GI, Kustatscher G, Buhecha HR, Allen MD, Pugieux C, Sait F, Bycroft M, Ladurner AG. The macro domain is an ADP-ribose binding module. EMBO J. 2005; 24:1911–1920. [PubMed: 15902274]

Levaot N, Simoncic PD, Dimitriou ID, Scotter A, La Rose J, Ng AH, Willett TL, Wang CJ, Janmohamed S, Grynpas M, et al. 3BP2-deficient mice are osteoporotic with impaired osteoblast and osteoclast functions. J Clin Invest. 2011; 121:3244–3257. [PubMed: 21765218]

Lietman SA, Kalinchinko N, Deng X, Kohanski R, Levine MA. Identification of a novel mutation of SH3BP2 in cherubism and demonstration that SH3BP2 mutations lead to increased NFAT activation. Hum Mutat. 2006; 27:717–718. [PubMed: 16786512]

Pleschke JM, Kleczkowska HE, Strohm M, Althaus FR. Poly(ADP-ribose) binds to specific domains in DNA damage checkpoint proteins. J Biol Chem. 2000; 275:40974–40980. [PubMed: 11016934]

Sada K, Miah SM, Maeno K, Kyo S, Qu X, Yamamura H. Regulation of FcepsilonRI-mediated degranulation by an adaptor protein 3BP2 in rat basophilic leukemia RBL-2H3 cells. Blood. 2002; 100:2138–2144. [PubMed: 12200378]

Smith S, Giriat I, Schmitt A, de Lange T. Tankyrase, a poly(ADP-ribose) polymerase at human telomeres. Science. 1998; 282:1484–1487. [PubMed: 9822378]

Talamonti MS, Roh MS, Curley SA, Gallick GE. Increase in activity and level of pp60c-src in progressive stages of human colorectal cancer. J Clin Invest. 1993; 91:53–60. [PubMed: 7678609]

Tiziani V, Reichenberger E, Buzzo CL, Niazi S, Fukai N, Stiller M, Peters H, Salzano FM, Raposo do Amaral CM, Olsen BR. The gene for cherubism maps to chromosome 4p16. Am J Hum Genet. 1999; 65:158–166. [PubMed: 10364528]

Ueki Y, Lin CY, Senoo M, Ebihara T, Agata N, Onji M, Saheki Y, Kawai T, Mukherjee PM, Reichenberger E, et al. Increased myeloid cell responses to M-CSF and RANKL cause bone loss and inflammation in SH3BP2 “cherubism” mice. Cell. 2007; 128:71–83. [PubMed: 17218256]

Ueki Y, Tiziani V, Santanna C, Fukai N, Maulik C, Garfinkle J, Ninomiya C, doAmaral C, Peters H, Habal M, et al. Mutations in the gene encoding c-Abl-binding protein SH3BP2 cause cherubism. Nat Genet. 2001; 28:125–126. [PubMed: 11381256]

Wiener JR, Windham TC, Estrella VC, Parikh NU, Thall PF, Deavers MT, Bast RC, Mills GB, Gallick GE. Activated SRC protein tyrosine kinase is overexpressed in late-stage human ovarian cancers. Gynecol Oncol. 2003; 88:73–79. [PubMed: 12504632]

Yeh TY, Beiswenger KK, Li P, Bolin KE, Lee RM, Tsao TS, Murphy AN, Heveer AL, Chi NW. Hypermetabolism, hyperphagia, and reduced adiposity in tankyrase-deficient mice. Diabetes. 2009; 58:2476–2485. [PubMed: 19651815]

Zhang Y, Liu S, Mickanin C, Feng Y, Charlat O, Michaud GA, Schirle M, Shi X, Hild M, Bauer A, et al. RNF146 is a poly(ADP-ribose)-directed E3 ligase that regulates axin degradation and Wnt signalling. Nat Cell Biol. 2011; 13:623–629. [PubMed: 21478859]

Highlights

- Cherubism-causing mutations in 3BP2 abolish recognition by Tankyrase
- ADP-ribosylation couples to ubiquitylation to control 3BP2 steady state levels
- Stabilization of 3BP2 protein accounts for dominant inheritance of cherubism
- Tankyrase represses SRC activation and TNFα induction in macrophages and osteoclasts

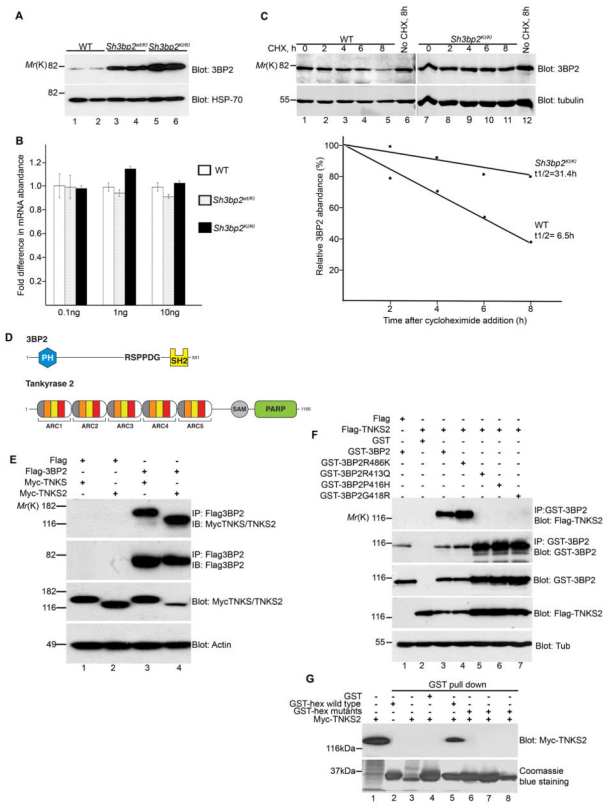

Figure 1. 3BP2 cherubism mutant protein is stabilized

(A) 3BP2 protein expression in macrophages derived from wild type (WT), *Sh3bp2*$^{KI/+}$, or *Sh3bp2*$^{KI/KI}$ mice was determined by Western blot analysis. (B) Quantitative PCR of *sh3bp2* mRNA derived from WT, *Sh3bp2*$^{KI/+}$, or *Sh3bp2*$^{KI/KI}$ macrophages. (C) Cycloheximide chase to ascertain 3BP2 protein stability in WT or *Sh3bp2*$^{KI/KI}$–bone marrow-derived macrophages (BMMs). BMMs obtained from either WT or *Sh3bp2*$^{KI/KI}$ mice, were treated with cycloheximide for the indicated time intervals, lysed and 3BP2 protein levels determined by Western blot analysis. The percentage of 3BP2 protein levels were plotted as a function of time. (D) 3BP2 and TNKS2 domain organization. 3BP2 is a PH- and SH2- domain containing adapter protein. The RSSPDG sequence mutated in cherubism patients is shown. TNKS2 contains five repeat clusters (ARCs), a Sterile Alpha Motif (SAM) domain and the PARP domain. (E) 3BP2 bind both TNKS and TNKS2. Myc-Tankyrase Western blot of Flag-3BP2 immune complexes expressed in HEK293T cells. (F) 3BP2 but not cherubism mutants bind to TNKS2. Tankyrase Western blot of GST-3BP2 and GST-3BP2 cherubism mutant immune complexes. (G) The 3BP2 targeting peptide (Hex) is sufficient to bind to TNKS2. Immobilized GST, GST-Hex(WT) or GST-Hex cherubism mutations R413Q, P416H or G418R were incubated with lysates from HEK293T cells over-expressing Myc-TNKS2 and probed for Myc-TNKS2 by Western blot. The levels of the recombinant GST-Hex peptide were evaluated by Coomassie staining. See also Figure S1

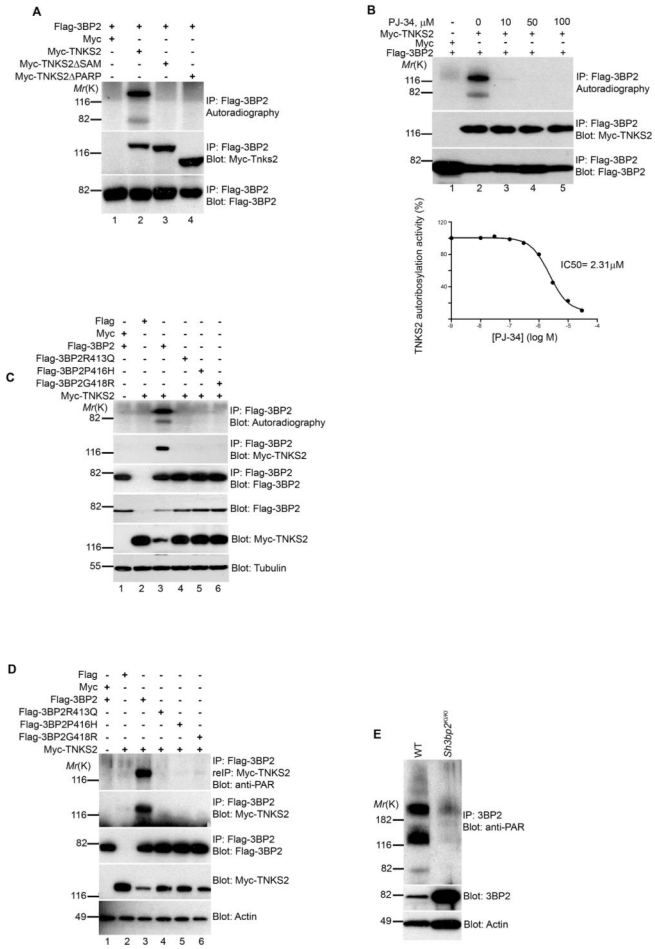

Figure 2. 3BP2 is ADP-ribosylated by TNKS2 *in vitro and in vivo*

(A) Ribosylation of 3BP2 and TNKS2 *in vitro* require the SAM and PARP domains of TNKS2. Flag-3BP2 immune complexes were subjected to an *in-vitro* PARP reaction using [^{32}P]NAD^{+}. Proteins were separated by SDS-PAGE and visualized by autoradiography. (B) The PARP inhibitor, PJ-34 inhibits TNKS2-dependent ribosylation of 3BP2. Flag-3BP2 immune complexes were subjected to an *in vitro* PARP reaction in the presence of increasing concentration of PJ-34. Lower panel, quantified inhibition of TNKS2 PARP activity by PJ-34, as evaluated by Myc-TNKS2 auto-ribosylation. (C) 3BP2 but not cherubism mutants of 3BP2 are ribosylated by TNKS2. Flag-3BP2 or Flag-3BP2 cherubism mutants were subjected to an *in vitro* PARP reaction. Ribosylation was measured by autoradiography. (D) Ribosylated TNKS2 is present in 3BP2 but not cherubism mutant protein complexes. Flag-3BP2 and Myc-TNKS2 were co-expressed in HEK293T cells. Flag-3BP2 protein complexes were dissociated in 1% SDS heated to 68°C then subjected to reprecipitation with an anti-Myc antibody and probed with an anti-poly(ADP-ribose) (PAR) antibody. (E) Endogenous 3BP2 but not a cherubism mutant is ribosylated in primary osteoclasts. Western blot of 3BP2 immune complexes derived from WT or *Sh3bp2*$^{KI/KI}$ bone marrow-derived osteoclasts were probed with anti-PAR specific antibodies. See also Figure S2.

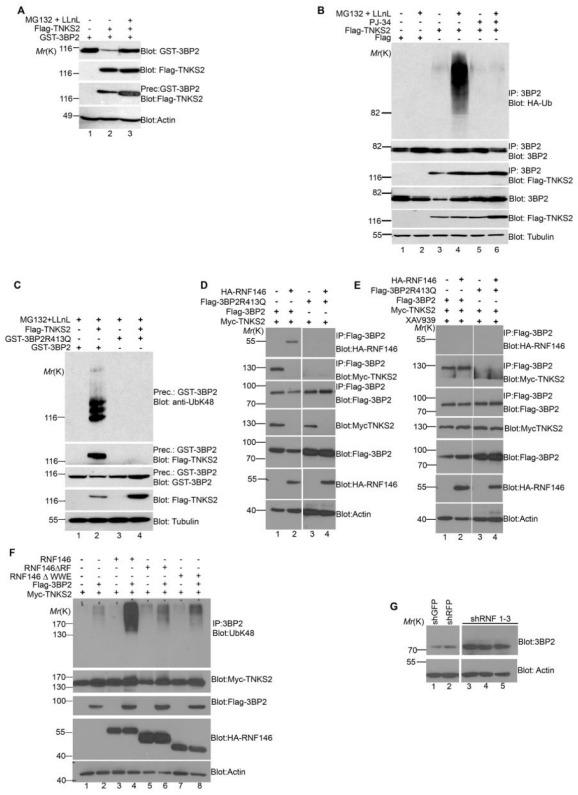

Figure 3. TNKS2 controls 3BP2 protein levels through ubiquitin-mediated proteolysis

(A) Proteasome inhibition by MG132 and LLnL reverses TNKS2-dependent suppression of 3BP2 protein levels. (B) Ubiquitylation of 3BP2 is stimulated by TNKS2 and requires PARP activity. HEK293T cells were transfected with TNKS2 and HA-Ubiquitin and incubated with proteosome or PARP inhibitors as indicated. Endogenous 3BP2 was immunoprecipitated and probed for HA-Ubiquitin. (C) TNKS2 stimulates ubiquitin-K48 modification of 3BP2. GST-3BP2 or GST-3BP2R413Q were expressed in HEK293T in the absence or presence of TNKS2. GST-3BP2 proteins were precipitated and probed with anti-UbK48 specific antibodies. (D) The E-3 ubiquitin ligase RNF146 binds to 3BP2 but not a cherubism mutant. Flag-3BP2 or Flag-3BP2R413Q immune complexes were probed for HA-RNF146 or Myc-TNKS2. The levels of protein expression for each condition are indicated in the panels below. (E) Binding of RNF146 to 3BP2 is ADP-ribosylation dependent. Flag-3BP2 or Flag-3BP2R413Q immune complexes derived from cells cultured in the presence of Tankyrase inhibitor XAV-939 were probed for HA-RNF146 or Myc-TNKS2. (F) Ubiquitylation of 3BP2 requires the ring finger and the WWE domain of RNF146. HA-RNF146 but not HA-RNF146ΔWWE or HA-RNF146ΔRF mutants induce 3BP2 ubiquitylation. HA-RNF146, HA-RNF146ΔWWE or HA-RNF146ΔRF were co-expressed with Flag-3BP2 and Myc-TNKS2. Flag-3BP2 immune complexes where probed with anti-UbK48 specific antibodies (G) Depletion of RNF146 stabilizes 3BP2 protein levels. HEK293T cells were transfected with one of three individual shRNAs targeting RNF146 (shRNF1–3) or two non-specific shRNAs. Endogenous 3BP2 and actin proteins were probed by Western blot. See also Figure S3.

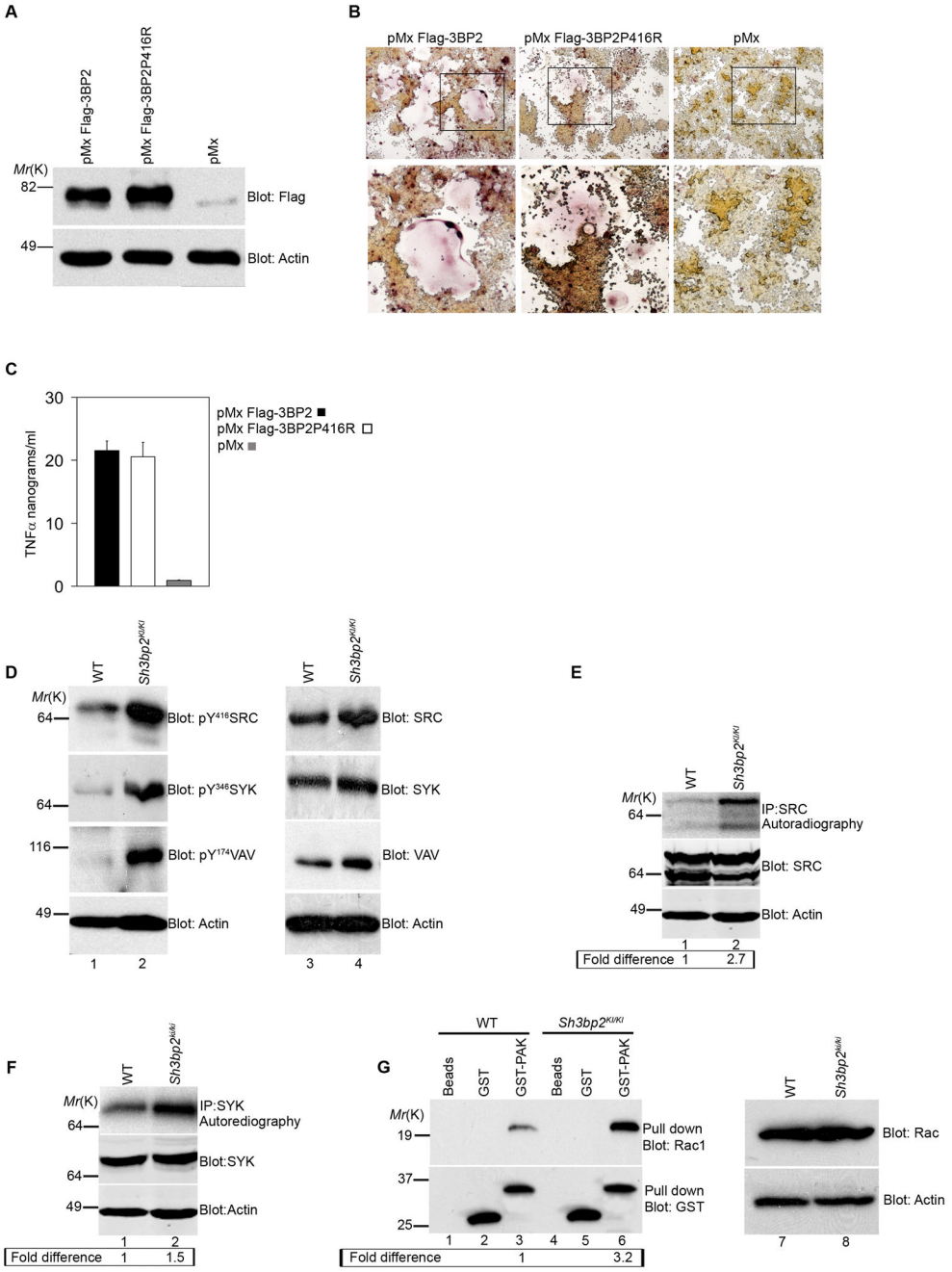

Figure 4. Elevated levels of wild type 3BP2 protein are sufficient to induce enhanced osteoclast formation and TNFα secretion by macrophages

(A) Lysates from RAW264.7 cell infected with retroviruses expressing WT Flag-3BP2, Flag-3BP2P416R, or empty vector were probed with anti-Flag antibodies. (B) TRAP positive multinucleated osteoclast cells derived from RAW264.7 infected cells as in (A). Images obtained using a Leica inverted microscope with 5X objectives. (C) TNFα levels in supernatants from RAW264.7 infected cells as in (A) from four independent experiments are shown. (D) SRC, SYK and VAV are hyper-phosphorylated in *Sh3bp2*$^{KI/KI}$ osteoclasts. Lysates from osteoclasts derived from WT or *Sh3bp2*$^{KI/KI}$ mice were probed with phospho-specific antibodies against SRC, SYK or VAV (left panel). The total protein levels are

shown respectively on the right panel. (E) SRC kinase activity is elevated in *Sh3bp2*$^{KI/KI}$ osteoclasts. Bone marrow-derived osteoclasts from either WT (lane 1) or *Sh3bp2*$^{KI/KI}$ (lane 2) were lysed and subjected to a SRC-specific immune complex *in vitro* kinase reaction. The specific kinase activity was calculated as the ratio of the autophosphorylation signal to the level of SRC expression. (F) SYK immune complex *in vitro* kinase reaction performed as in (E). (G) RAC-GTP levels are elevated in *Sh3bp2*$^{KI/KI}$ osteoclasts. RAC-GTP levels in osteoclasts derived WT or *Sh3bp2*$^{KI/KI}$ mice were measured using a PAK GST-PBD pull-down assay. RAC-GTP levels in the WT osteoclasts were normalized to 1 and RAC-GTP levels in *Sh3bp2*$^{KI/KI}$ osteoclasts expressed as fold difference compared to WT values.

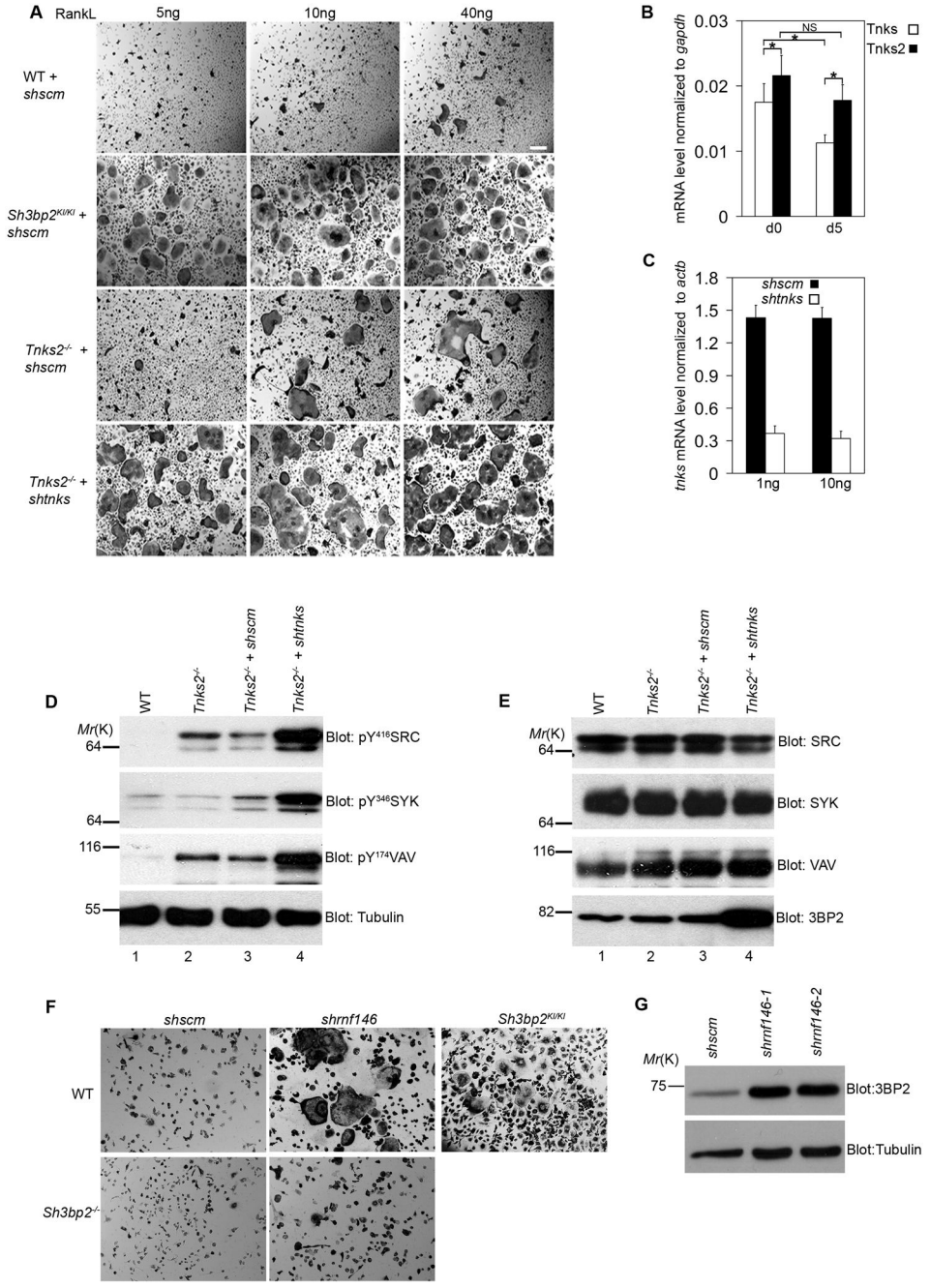

Figure 5. Primary bone marrow-derived macrophages depleted of TNKS/TNKS2 undergo accelerated osteoclastogenesis

(A) TNKS/TNKS2-deficient osteoclasts phenocopy cherubism osteoclasts. BMMs from WT, *Sh3bp2*$^{KI/KI}$, or *Tnks2*$^{-/-}$ mice were infected with scrambled shRNA retrovirus (first three rows). BMMs derived from *Tnks2*$^{-/-}$ mice were infected with *tnks*-specific shRNA retrovirus (fourth row). Cells were then grown in CSF-1 (30 ng/ml) and RANKL (5 ng/ml, 10 ng/ml or 40 ng/ml) for three days to initiate osteoclastogenesis, then TRAP stained. Experiments were performed in triplicate. Scale bar: 50μm. (B) Both *tnks* and *tnks2* mRNA are expressed in osteoclasts. Tankyrase mRNA levels in BMMs cultured in RANKL and CSF-1 as determined by qPCR at day 0 and day 5. *P<0.05; NS, no statistical significance.

(C) *tnks* mRNA levels in *Tnks2*$^{-/-}$ osteoclasts infected with scrambled or *tnks*-specific shRNA retrovirus as determined by qPCR. (D–E) TNKS/TNKS2-depleted osteoclasts express elevated levels of phosphorylated SRC, SYK and VAV and increased levels of 3BP2 protein. Lysates from primary osteoclasts in (A) were probed with phospho-specific antibodies against SRC, SYK, or VAV (D). The total protein levels as determined by Western blot are shown (E). (F) RNF146-deficient osteoclasts phenocopy cherubism osteoclasts. BMMs from WT or *Sh3bp2*$^{-/-}$ mice infected with scrambled shRNA or RNF146 specific shRNA, were grown in CSF-1 (30 ng/ml) and RANKL (5 ng/ml) for three days then TRAP stained. Cultured osteoclasts from *Sh3bp2*$^{KI/KI}$ mice are shown for comparison. Experiments were performed in triplicate. Scale bars: 50μm. (G) RNF146-depleted osteoclasts express elevated levels of 3BP2. Lysates from primary osteoclasts expressing two different RNF146-targeting shRNAs (*shrnf146-1 and shrnf146-2*) or a scrambled shRNA (*shscm*) were probed for 3BP2 protein expression by Western blot. See also Figure S4.

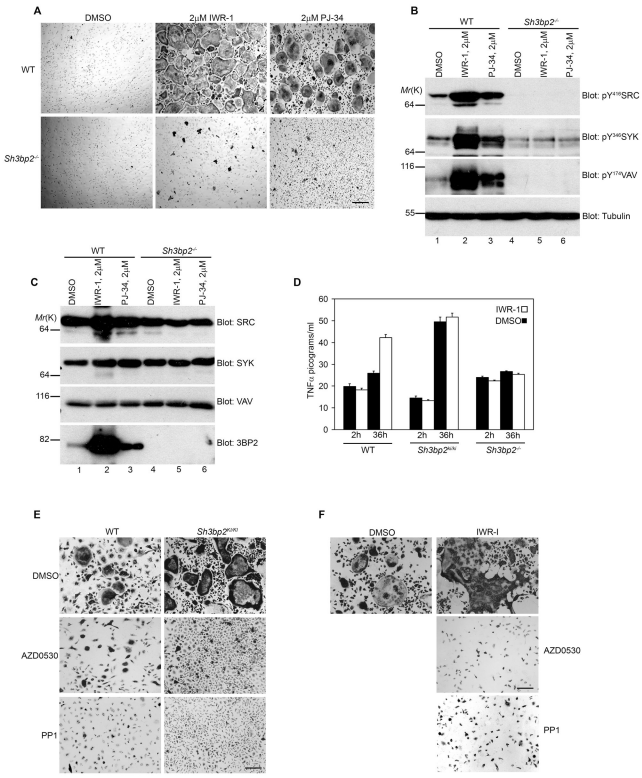

Figure 6. Tankyrase inhibition enhances osteoclastogenesis in a 3BP2 dependent manner

(A) BMMs harvested from WT or *Sh3bp2*$^{-/-}$ mice were grown under osteoclastogenic conditions in the presence of IWR-1 (2 μM) or PJ34 (2 μM) and then TRAP-stained. Scale bars: 50μm. (B and C). Osteoclasts grown in the presence of the IWR-1 or PJ34 express elevated levels activated SRC, SYK and VAV and increased protein levels of 3BP2. Lysates from cells treated as in (A) were blotted with phospho-specific antibodies against SRC, SYK, or VAV as in Figure 5D. (C) SRC, SYK, VAV and 3BP2 protein levels as determined by Western blot are shown. (D) TNFα levels in the supernatant of primary macrophages incubated for the indicated times with CSF-1 in the presence or absence of IWR-1 (2μM). (E) BMMs harvested from WT and *Sh3bp2*$^{KI/KI}$ mice were cultured under osteoclastogenic conditions in the presence of the SRC inhibitors AZD0530 (0.5 μM) or PP1 (5 μM) then TRAP-stained. Scale bars: 50μm. (F) WT BMMs were cultured under osteoclastogenic condition in the presence of IWR-1 and either AZD0530 (0.5 μM) or PP1 (5 μM) then TRAP-stained. Scale bars: 50μm.

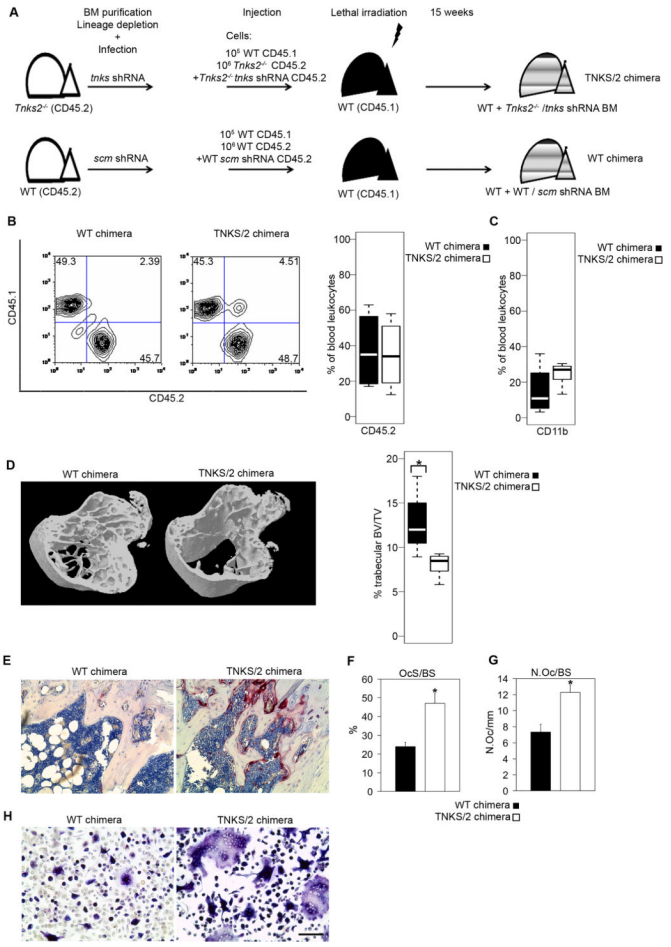

Figure 7. Radiation chimeric mice, which lack Tankyrase phenocopy features of cherubism

(A)10^6 *Tnks2*$^{-/-}$ lineage-depleted bone marrow cells (C57Bl/6, CD45.2) were infected with a lentivirus harboring a *Tnks*-specific shRNA and then injected together with 10^5 CD45.1 WT bone marrow cells into lethally irradiated, syngeneic (CD45.1) recipients (**TNKS/2 chimera**). WT control chimeric mice were generated from CD45.2-derived bone marrow cells infected with a lentivirus expressing a scrambled shRNA hairpin (**WT chimera**). (B) Fifteen weeks following transplantation engraftment was measured by the percentage of CD45.2 positive leukocytes in the peripheral blood. (C) Percentage of donor monocytes ($CD45.2^+CD11b^+$) in chimeric mice is shown. WT, n=4; TNKS/2, n=5; *, p<0.16. (D)μCT reconstruction of the trabecular bone of WT or TNKS/2 chi meric mice 15 weeks after injection (left). μCT-derived measurements of the trabecular bone volume fraction (BV/TV) (right).WT, n=4 and TNKS/2, n=5; *P< 0.05. (E) TRAP staining of tibia of WT and TNKS/2 chimeric mice. Histomorphometric analysis of (F) osteoclast surface to bone surface (OcS/BS) and (G) osteoclast number to bone perimeter (N.Oc/BS) in the tibias of WT and TNKS/2 chimeric mice 15 weeks after transplantation of donor cells. n=3 WT and n=5 TNKS/2. *P< 0.01. (H) BMMs harvested from WT or TNKS/2 chimeric mice were grown under osteoclastogenic conditions and TRAP-stained. Scale bars: 50μm. See also Figure S5.